

A Color Cast Image Enhancement Method based on Affine Transform in Poor Visible Conditions

Zheng Liang, Xueyan Ding, Jie Jin, Yafei Wang, Yulin Wang, Xianping Fu

Abstract—In this letter, a simple yet effective dehazing framework is proposed, which consists of a novel color correction and a contrast enhancement. Most of the existing dehazing works focus on enhancing the contrast of the degraded images, but rarely of them concern about the color cast, which are ubiquitous in scattering medium. To address the color distortion, an affine transform model-based color correction method is firstly proposed to improve the appearance of image while preserving the details, which is inspired by the traditional color transfer. The color transfer alters the color values of a source image by sharing the global color statistics of a reference image, which makes it unsuitable to address the locally variable color deviations encountered in highly color distorted images as in poor visible conditions (sandstorms, underwater). To alter color correction locally, we add local color fidelity and gradient constraint to the proposed technique, which overcomes the limitation that the traditional method depends too much on the global color statistics of the reference image and encourages it to handle the degraded image with various color casts and light conditions. In addition, a multi-scale gradient domain processing is applied to enhance the contrast. In this procedure, by extracting the information of different layers, we can easily restore the contrast while limiting the significant amplification of noise. The extensive qualitative and quantitative experiments reveal that the color and the contrast can be significantly improved by the proposed technique.

Index Terms—color cast, color transfer, contrast enhancement.

I. INTRODUCTION

MOST computer vision methods require that the input image is of scene content that are clear and visible. However, during the optical imaging in poor visible conditions, due to the scattering effect and the absorption effect, the propagated light suffers from high attenuation, which causes the recorded images generating severe color distortion, low contrast and noise. These poor visibility limits the application performance of them in object detection and remote sensing.

Over the past few decades, various methods [1]–[14] are introduced to improve the quality of such degraded images. Single image-based techniques often rely on kinds of assumptions and priors, the well-known Dark Channel Prior (DCP) [1] is the most representative one. Inspired by the prior, the method of Li et al. [8] yield superior results than conventional

This work was supported in part by the National Natural Science Foundation of China Grant 61802043 and Grant 62002043, by the Liaoning Revitalization Talents Program Grant XLYC1908007, by the Dalian Science and Technology Innovation Fund 2019J11CY001. (Corresponding author: Xianping Fu.)

Z. Liang and X. Ding contributed equally to this work.

Zheng Liang is with the School of Internet, Anhui University, Hefei 230039, China. Other authors are with the School of Information Science and Technology, Dalian Maritime University, Dalian 116026, China.(e-mail: zliang@ahu.edu.cn, {dingxueyan, jjie, wangyafei, yl_wang, fxp}@dlmu.edu.cn).

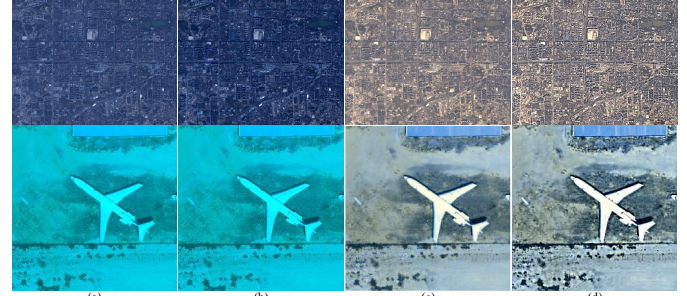


Fig. 1. The first column shows the raw images captured under challenging extreme scenes such as sandstorm. The second column is the results yielded by employing the well-known DCP method [1]. As shown in the third column and the fourth column, benefiting from the proposed method, the color and the contrast of the degraded images are naturally restored.

dehazing or stereo techniques by employing DCP and other depth cues from stereo matching. Additionally, with the success development of deep learning in computer vision, more and more deep learning-based methods are applied to restore the degraded images. An AOD-Net of Ref. [10] is proposed to learn a mapping function between the hazy image and the haze-free image directly. Ren et al. [15] propose a multi-scale CNN (MSCNN) to generate a coarse-scale transmission matrix and gradually refined it. Although deep-learning based dehazing approaches achieved impressive performance, the insufficiency of labeled training data severely limits the further development of these methods. To overcome this limitation, more and more works [16], [17] are presented to construct the large-scale image datasets in recent years.

Algorithm 1: The outline of the proposed technique

Input: Source image S , Reference image R ;

Output: Output image Z .

1. Calculate the covariance C_S of the source image;
 2. Calculate the covariance C_R of the reference image;
 3. Minimize the object fuction Eq.7 by gradient descent;
 4. Obtain the color corrected image Y using Eq.2;
 5. Estimate the transmission t using the method introduced by [18];
 6. Covert the image Y form RGB to CIELAB
 7. Obtain the progressively coarser version of the lightness channel L by WLS [19];
 8. Obtain the detail layers d_1 and d_2 using Eq.14;
 9. Reconstruct the detail layers d'_1 and d'_2 using Eq.12;
 10. Obtain the Reconstructed image L_R using Eq.15;
 11. Yield the finally enhanced image by converting the CIELAB to RGB.
-

Most of the existing image restoration works might tend to

enhance the contrast without considering the color distortion, leading to the inaccurate restoration results (as shown in Fig.1). In particular, if one color channel is highly attenuated for images taken under challenging scenes, the color compensation is a vital pre-processing procedure, which is often ignored in most of the existing image dehazing methods, especially in land-based image dehazing. Therefore, this letter firstly proposes an affine transform model-based color correction method as the pre-processing procedure, which is inspired by the color transfer method. The proposed method overcomes the main limitation that the conventional color transfer relies too much on the global information from the reference image through blending local color and global covariance mapping, which makes it to robustly process the degraded images with different color tones. Additionally, a multi-scale process is applied to enhance the contrast while limiting the significant amplification of noise. The outline of the proposed technique is presented in Algorithm.1.

II. PROPOSED METHODOLOGY

A. Motivation

The method of Reinhard et al. alters the pixel values of the source image by matching the means and the standard deviations of the source image and the reference image in the $\alpha\beta$ color space, which can be formulated by [20]:

$$I_{CT}^c(x) = \frac{\sigma_R^c}{\sigma_S^c} (I_S^c(x) - \bar{I}_S^c) + \bar{I}_R^c \quad (1)$$

where indicators CT , R and S are the color transferred image, the reference image and the source image, respectively. x is the coordinate of pixel, $c \in (l, \alpha, \beta)$, \bar{I}_S^c and \bar{I}_R^c refer to the mean value of color component c in the source and the reference image, respectively. σ_S^c and σ_R^c indicate the standard deviation in the source and the reference image, respectively.

B. Color correction

The degraded images are often characterized by color distortion and low brightness which results from various illumination and medium attenuation properties. In the proposed framework, color correction is firstly proposed to restore the natural appearance of the degraded images. The color correction method is based on a simple affine transform model, which inspired by the equation of the traditional color transfer as shown in Eq.1. The affine model can be written as:

$$Y = MX + N \quad (2)$$

where X and Y denote the source image and the corrected image, M and N are two transferred coefficients. An ideal color transfer technique should maintain the scene from the input image and match the color style of the reference image, so we firstly constraint the local fidelity between the input image and the corrected image, which can be expressed by:

$$Q^{fidelity} = \|MX + N - Y\|_F^2 \quad (3)$$

In this method, the color covariance C_S of the source image and the color covariance C_R of the reference image are known. Combining the proposed affine model $Y = MX + N$ with the color covariance C_S of the source image X , the color variance



Fig. 2. The corrected underwater images. (a) Original image. (b) Corrected image without the gradient constraint. (c) Corrected image with the gradient constraint. (d) Reference image in this letter.



Fig. 3. The corrected underwater images. (a) Original image. (b) R channel with high attenuation. (c) G channel. (d) B channel. (e) Corrected image without the boundary constraint. (f) Corrected image with the boundary constraint.

of the corrected image Y can be deduced as $MC_S M^\top$. To match the color style of the reference image, the covariance of the corrected image should be as close as that of the reference, we propose a regularizer to constraint the covariance of the output image, it can be expressed as:

$$Q^{covariance} = \|MC_S M^\top - C_R\|_F^2 \quad (4)$$

In addition, to preserve the detail information of the input image during transfer process, an additional gradient regularizer is also taken into account

$$Q^{gradient} = \|M(DX) - DX\|_F^2 \quad (5)$$

where D is the difference operators, DX denotes the gradient of the input image, and $M(DX)$ refers to the gradient of the output image under the affine transform model. As shown in Fig.2, the detail and outline are more clearer in the corrected image yielded by using the proposed gradient regularizer. If only introducing the above regularization constraint terms, the method may still suffer from poor performance in robustness. This is because some channels may be highly attenuated in some images, only applying the above regularizers may result into having larger value for the affine model parameter in trying to match them to follow the local mapping or the global pixel covariance, which results into artifacts saturating the output image into one color. As shown in Fig.3, the red channel suffers from extreme attenuation, using the above regularization constraints may introduce the reddish in the result. Thus, to maintain the bounded energy of the affine transform, another regularizer is also added as follows:

$$Q^{boundary} = \|M\|_F^2 + \|N\|_2^2 \quad (6)$$

Different from some previous works that relied on global covariance information from the reference, the main goal of our technique is to seek the best solution of parameters M and N for blending the local color mapping and the global color covariance mapping. With the help of these regularization constraints, we can achieve objective by using the given equation as:

$$(M^*, N^*) = \arg \min_{M, N} \left\{ \|MX + N - Y\|_F^2 + \frac{\lambda}{2} \|MC_S M^\top - C_R\|_F^2 + \beta \|M(DX) - DX\|_F^2 + \frac{\gamma}{2} (\|M\|_F^2 + \|N\|_2^2) \right\} \quad (7)$$

where λ , β and γ are three positive parameters that control the importance of different terms ($\lambda = 0.5$, $\beta = 1$ and $\gamma = 0.5$ in



Fig. 4. Comparative results of different color correction methods. These corrected images yielded by using Gray-world [21], Grey-edge [22], the more recent methods of Song et al. [23], Fu et al. [24], Mi et al. [25] and ours, respectively.

TABLE I

BLUR AND CCF VALUES OF DIFFERENT METHODS IN FIG.4.

	Gray-world [21]	Grey-edge [22]	Song [23]	Fu [24]	Mi [25]	Our						
	Entropy	UCIQE	Entropy	UCIQE	Entropy	UCIQE						
(a)	7.54	0.52	6.89	0.41	6.28	0.42	7.16	0.62	7.51	0.59	7.70	0.55
(b)	7.27	0.46	7.43	0.46	7.60	0.48	7.49	0.50	7.65	0.52	7.67	0.49

this letter). To obtain the optimal solution of Eq.7, we simply solve the problem using gradient descent.

$$M^* = 2(MX - Y + N)X^T + 2\lambda MC_S M^T MC_S \\ - 2\lambda C_R MC_S + \gamma M + 2\beta(M(DX) - DX)(DX)^T \quad (8)$$

$$N^* = 2(MX - Y + N) + \gamma N \quad (9)$$

Fig.4 shows two visual comparative samples. On the provided underwater images, we applied the following methods: the classical Gray-world technique [21], Grey-edge technique [22], but also the more recent methods of Song et al. [23], Fu et al. [24], Mi et al. [25] and ours, respectively. As can be observed that Max-rgb and Grey-edge are not able to remove entirely the casts. The results of Gray-world suffer from reddish, and the results of Song et al. and Fu et al. are also not able to restore the correct colors, such as the white sands. The color of the resultant image yielded by Mi et al. is over-corrected. In addition, we use Entropy and UCIQE [26] to quantitatively assess the effectiveness of various color correction techniques. The quantitative values are listed in Table.I and the values in bold denote the best results. As performed in Table.I, the proposed method achieves the highest Entropy values, which means that the proposed method generally results in better appearance, with sufficient restoration of the color and the structure. Although the UCIQE of our method is the third-best performer, as can be seen from Fig.4 (a) that the higher UCIQE values do not provide the better subjectively quality, since it is demonstrated that UCIQE might be biased to some characteristics (not entire image) and did not take the color distortion and brightness into account in [17]. Overall, our technique shows the highest performance in preserving the color appearance.

C. Contrast enhancement

The atmospheric scattering model can be expressed by [1]:

$$Y(x) = Z(x)t(x) + A(1 - t(x)) \quad (10)$$

where Y and Z are the input image and the haze-free image, respectively. t denotes the transmission and A is the global backscattered light. We assumed that the values of scene depth and attenuation coefficient within a small local patch centered at location x are constant, the transmission t is uniform and the contrast of the input image can be written by [1]:

$$\sum_x \|\nabla Y(x)\| = \sum_x \|t \nabla Z(x) + (1 - t) \nabla A\| \\ = t \sum_x \|\nabla Z(x)\| \quad (11)$$

∇ denotes the gradient operator. This equation indicates that we can easily enhance the contrast on gradient domain of multi-scale detail layers of the input image, which can be formulated by:

$$\nabla d'_i = \frac{\omega_i}{\bar{t}} \nabla d_i \quad (12)$$

where d_i and d'_i are the i_{th} detail layer and the i_{th} enhanced detail layer, respectively. ω_i are the parameters used to control the enhancement strength of gradient. \bar{t} is the mean value of the transmission t , in which t is estimated by the fast method introduced by [18]. To obtain the detail layers, we employ the weighted least squares (WLS) [19] in the lightness channel L of CIELAB color space of input image to make a multi-scale representation, which can be expressed by

$$u = F_\lambda(L) = (I + \lambda K_L)^{-1} L \quad (13)$$

where u denotes the smoothed version of L , I is the identity matrix. $K_L = D_h^T A_h D_h + D_v^T A_v D_v$, in which D_h and D_v represent the discrete differentiation operation, A_h and A_v contain the smoothness weights. By increasing the λ value in Eq.13, the progressively smoothed version u^1, u^2, \dots, u^{k-1} can be obtained, and we define the coarsest version u^{k-1} of the input image L as the base layer b and the detail layers d_i can be obtained as:

$$d_i = u^{i-1} - u^i, \text{ where } i = 1, \dots, k-1 \text{ and } u^0 = g \quad (14)$$

where k is set to 3 in this letter, since we observed that $k=3$ can obtain the satisfied performance and the greater values of k does not imply significant improvement, but indicates the higher computational complexity. After getting the detail layers d_1 and d_2 , the reconstructed layers d'_1 and d'_2 can be obtained using Eq.12 ($\omega_1 = 1, \omega_2 = 2$) and solving a Poisson equation [25]. Accordingly, the reconstructed L image is given as:

$$L_R = b + d'_1 + d'_2 \quad (15)$$

The finally enhanced image can be obtained by converting the CIELAB image to RGB image.

III. EXPERIMENT RESULTS AND DISCUSSION

To validate the effectiveness of our technique, we compare it with several state-of-the-art works on both land-based images and underwater images. All these tested land-based images are collected from Internet and underwater images are provided by RUIE dataset [27]. The source codes of the competitive methods are provided by authors or GitHub.

A. Validation on Land-based Image

To verify the effectiveness of our dehazing method on remotely sensed land-based images, we first qualitatively compare the proposed method with several specialized land-based image dehazing methods (He et al. [1], Peng et al. [28], Zhu et al. [29], Meng et al. [6], Shin et al. [30], Colores et al. [31], Qin et al. [32], Cho et al. [33]). Fig.5 shows the resultant images yielded by our approach and these competitive methods. As we can observe that the raw images are characterized by different color tones and non-uniform illumination conditions. The methods of He et al. [1], Qin et al. [32] and Zhu et al. [29] are not able to remove the haze

TABLE II
̄ AND σ VALUES OF DIFFERENT METHODS IN FIG.5.

	He [1]	Peng [28]	Zhu [29]	Meng [6]	Shin [30]	Colores [31]	Qin [32]	Cho [33]	OPP	Our (-w/o OPP)	Our
	\bar{r}	Blur	\bar{r}	Blur	\bar{r}	Blur	\bar{r}	Blur	\bar{r}	Blur	\bar{r}
(a)	1.770	0.349	2.659	0.368	0.978	0.313	6.113	0.300	1.864	0.273	2.347
(b)	0.972	0.279	1.717	0.240	0.999	0.273	2.002	0.266	1.476	0.250	1.721
(c)	0.990	0.275	2.219	0.255	0.987	0.273	2.497	0.272	1.168	0.310	1.936
(d)	1.704	0.351	3.236	0.361	0.964	0.352	4.508	0.317	2.605	0.347	3.141
(e)	1.301	0.274	3.004	0.274	0.957	0.259	1.417	0.280	1.025	0.259	2.068
(f)	1.345	0.221	3.312	0.208	0.549	0.221	1.195	0.211	2.237	0.214	2.143
(g)	1.147	0.337	1.625	0.303	0.916	0.344	2.359	0.308	2.062	0.317	1.676
(h)	1.048	0.218	2.081	0.211	0.829	0.203	1.307	0.202	2.239	0.210	1.229

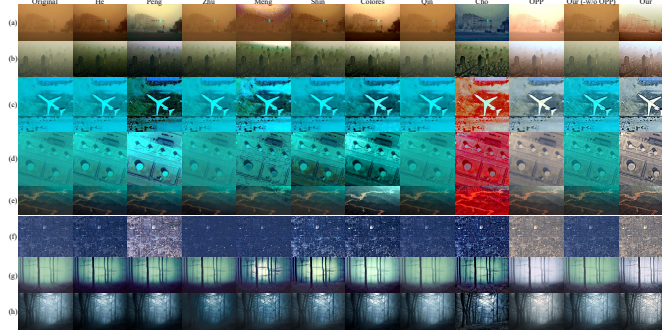


Fig. 5. Qualitative comparative results on various remotely sensed land-based images. The rows from left to right show the original images, the resultant images of He et al. [1], Peng et al. [28], Zhu et al. [29], Meng et al. [6], Shin et al. [30], Colores et al. [31], Qin et al. [32], Cho et al. [33], Our pre-processing, Ours (-w/o OPP) and Our method, respectively.

and correct the color distortion. Although the approaches of Peng et al. [28] and Meng et al. [6] are proven to be effective for few images, their methods almost introduce artificial light and color distortion. Shin et al.'s method [30]) can improve the overall quality. However, the dehazed images generated by their methods still suffer from lots of haze. The method of Cho et al. suffers from reddish. Although the proposed method without our pre-processing procedure (Ours (-w/o OPP)) and the method of Colores et al. [31] can improve the contrast, the color distortion is not removed. With the help of our pre-processing procedure , our method not only improves the visibility of the images but also yields an pleasing structure and vibrant yet genuine colors.

Then, we quantitatively evaluate the performance of different dehazing methods using two different metrics: Blur [34] and Blind contrast [35]. The blur metric validates the performance of the enhanced images in terms of blur perception. The lower value, the higher the image quality. The blind contrast metric contains three indicators: e , σ and \bar{r} . e measures the rate of new visible edges in the enhanced images, however, the spurious edges and artifacts may provide serious interference, we do not take the new visible edges indicator into account. σ denotes the percentage of saturated pixels while \bar{r} measures the quality of the contrast restoration. The values of σ is almost zero in most methods we compared, Therefore, we quantitatively evaluate the performance using Blur and \bar{r} , Good results are characterized by high scores of \bar{r} and low scores of Blur. The quantitative results are given in Table.II. As can be observed from these tables, our method stands out among these competitive methods. It should be noted that although the blur values of our method are higher than the methods of Shin et al. [30] and Meng et al. [6] in terms of Fig.5 (a) and Fig.5 (d), the visual quality of our method is much

TABLE III
̄ AND UCIQE VALUES OF DIFFERENT METHODS IN FIG.6.

	Peng [28]	Berman [36]	Li [37]	Li [17]	OPP	Our (-w/o OPP)	Our	
	\bar{r}	UCIQE	\bar{r}	UCIQE	\bar{r}	UCIQE	\bar{r}	UCIQE
(a)	2.03	0.59	1.84	0.59	5.93	0.64	1.65	0.51
(b)	1.38	0.55	1.94	0.63	2.12	0.64	1.33	0.52
(c)	1.46	0.54	1.13	0.61	1.42	0.62	1.07	0.55
(d)	1.32	0.53	3.38	0.54	1.37	0.60	0.94	0.53
(e)	1.62	0.53	1.33	0.63	1.04	0.53	1.10	0.54

TABLE IV
BLUR AND CCF VALUES OF DIFFERENT METHODS IN FIG.6.

	Peng [28]	Berman [36]	Li [37]	Li [17]	OPP	Our (-w/o OPP)	Our	
	Blur	CCF	Blur	CCF	Blur	CCF	Blur	CCF
(a)	0.452	22.81	0.39	31.87	0.31	44.91	0.52	15.89
(b)	0.19	32.42	0.17	40.58	0.18	47.91	0.19	21.08
(c)	0.26	31.29	0.24	43.62	0.24	35.76	0.27	26.21
(d)	0.26	30.25	0.33	20.38	0.25	36.28	0.26	26.39
(e)	0.24	35.41	0.22	38.90	0.25	29.46	0.26	24.63

better than them. And regarding the \bar{r} scores, our method is at least 20% better than the second-best performer in most cases. Additionally, the proposed color correction method employed as a pre-processing step, consistently improves the outcome of conventional restoration processes.

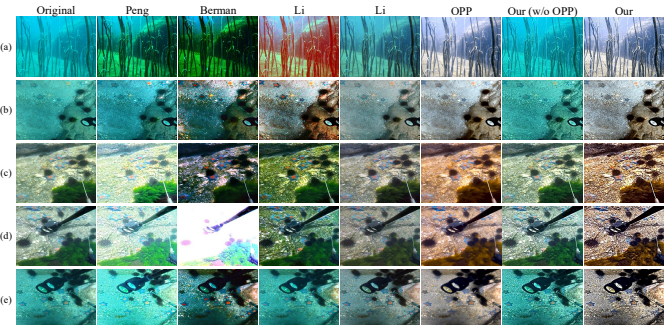


Fig. 6. Qualitative comparative results on underwater images. The rows from left to right show the original images, the resultant images of Peng et al. [28], Berman et al. [36], Li et al. [37], Li et al. [17], Our pre-processing, Ours (-w/o OPP) and Our method, respectively.

B. Validation on Underwater Image

To further prove the generalization of the proposed technique on underwater images, we also try to enhance underwater hazy images captured in real marine aquaculture environment and compare it with the approaches of Peng et al. [28], Berman et al. [36], Li et al. [37] and Li et al. [17]. Among these methods we tested, the techniques of Berman et al. [36], Li et al. [37] and Li et al. [17] are the specialized underwater image dehazing methods. We quantitatively evaluate the performace using the above mentioned indicator \bar{r} , Blur and the other two metrics (UCIQE [26] and CCF [38]) used to assess underwater image quality. UCIQE measures the chroma, saturation and contrast while CCF is a measurement of colorfulness, contrast, and fog density of an underwater image. The higher values of UCIQE and CCF, the better

image quality. Fig.6 shows the competitive results generated by different methods and the corresponding quantitative results are given in Table.III and Table.IV. As can be seen that the results of Peng et al. [28] and Li et al. [37] suffer from severe color cast. And the approach of Berman et al. [36] sometimes appears to generate the dark region. Overall, the resultant images of our approach are superior to other methods both in color and contrast.

IV. CONCLUSION

This letter proposes an efficient color cast image dehazing framework that consists of a novel affine transform-based color correction procedure and a multi-scale gradient domain contrast enhancement method. The color correction approach is firstly to remove the color distortion caused by hazy, sandy and water, and then, a contrast enhancement approach is applied to further enhance the contrast. The extensive validation reveals the proposed technique is effective.

Although the proposed method yields good performance among these images we tested, it is not without limitations. The expensive computational efficiency may be required in our method. Additionally, it is difficult to adaptively select the reference image. These limitations make the proposed method unsuitable for real-time applications, which need to be further improved in the future work.

REFERENCES

- [1] K. He, J. Sun, and X. Tang, "Single image haze removal using dark channel prior," *IEEE Trans. Pattern Anal. Mach. Intell.*, vol. 33, no. 12, pp. 2341–2353, 2010.
- [2] X. Fu, J. Wang, D. Zeng, Y. Huang, and X. Ding, "Remote sensing image enhancement using regularized-histogram equalization and dct," *IEEE Geosci. Remote Sens. Lett.*, vol. 12, no. 11, pp. 2301–2305, 2015.
- [3] F. A. Dharejo, Y. Zhou, F. Deeba, and Y. Du, "A color enhancement scene estimation approach for single image haze removal," *IEEE Geosci. Remote Sens. Lett.*, 2019.
- [4] M. Kaur, D. Singh, V. Kumar, and K. Sun, "Color image dehazing using gradient channel prior and guided l0 filter," *Information Sciences*, vol. 521, pp. 326–342, 2020.
- [5] A. M. Chaudhry, M. M. Riaz, and A. Ghafoor, "A framework for outdoor rgb image enhancement and dehazing," *IEEE Geosci. Remote Sens. Lett.*, vol. 15, no. 6, pp. 932–936, 2018.
- [6] G. Meng, Y. Wang, J. Duan, S. Xiang, and C. Pan, "Efficient image dehazing with boundary constraint and contextual regularization," in *Proc. IEEE ICCV*, 2013, pp. 617–624.
- [7] D. Singh, V. Kumar, and M. Kaur, "Image dehazing using window-based integrated means filter," *Multimedia Tools and Applications*, pp. 1–23, 2019.
- [8] Z. Li, P. Tan, R. T. Tan, D. Zou, S. Zhiying Zhou, and L.-F. Cheong, "Simultaneous video defogging and stereo reconstruction," in *Proc. IEEE CVPR*, 2015, pp. 4988–4997.
- [9] D. Singh and V. Kumar, "A novel dehazing model for remote sensing images," *Comput. Electr. Eng.*, vol. 69, pp. 14–27, 2018.
- [10] B. Li, X. Peng, Z. Wang, J. Xu, and D. Feng, "Aod-net: All-in-one dehazing network," in *Proc. IEEE ICCV*, 2017, pp. 4770–4778.
- [11] J. Li, K. A. Skinner, R. M. Eustice, and M. Johnson-Roberson, "Watrgan: Unsupervised generative network to enable real-time color correction of monocular underwater images," *IEEE Robot. Autom. Lett.*, vol. 3, no. 1, pp. 387–394, 2017.
- [12] C. Li, C. Guo, J. Guo, P. Han, H. Fu, and R. Cong, "Pdr-net: Perception-inspired single image dehazing network with refinement," *IEEE Trans. Multimedia*, vol. 22, no. 3, pp. 704–716, 2019.
- [13] C. Li, S. Anwar, J. Hou, R. Cong, C. Guo, and W. Ren, "Underwater image enhancement via medium transmission-guided multi-color space embedding," *IEEE Trans. Image Process.*, vol. 30, pp. 4985–5000, 2021.
- [14] N. Yang, Q. Zhong, K. Li, R. Cong, Y. Zhao, and S. Kwong, "A reference-free underwater image quality assessment metric in frequency domain," *Signal Process. Image Commun.*, vol. 94, p. 116218, 2021.
- [15] W. Ren, S. Liu, H. Zhang, J. Pan, X. Cao, and M.-H. Yang, "Single image dehazing via multi-scale convolutional neural networks," in *ECCV*. Springer, 2016, pp. 154–169.
- [16] B. Li, W. Ren, D. Fu, D. Tao, D. Feng, W. Zeng, and Z. Wang, "Benchmarking single-image dehazing and beyond," *IEEE Trans. Image Process.*, vol. 28, no. 1, pp. 492–505, 2018.
- [17] C. Li, C. Guo, W. Ren, R. Cong, J. Hou, S. Kwong, and D. Tao, "An underwater image enhancement benchmark dataset and beyond," *IEEE Trans. Image Process.*, vol. 29, pp. 4376–4389, 2019.
- [18] J.-P. Tarel and N. Hautiere, "Fast visibility restoration from a single color or gray level image," in *Proc. IEEE ICCV*, 2009, pp. 2201–2208.
- [19] Z. Farbman, R. Fattal, D. Lischinski, and R. Szeliski, "Edge-preserving decompositions for multi-scale tone and detail manipulation," *ACM Trans. on Graph.*, vol. 27, no. 3, pp. 1–10, 2008.
- [20] E. Reinhard, M. Adhikmin, B. Gooch, and P. Shirley, "Color transfer between images," *IEEE Comput. Graph. Appl.*, vol. 21, no. 5, pp. 34–41, 2001.
- [21] G. Buchsbaum, "A spatial processor model for object colour perception," *Journal of the Franklin institute*, vol. 310, no. 1, pp. 1–26, 1980.
- [22] J. Van De Weijer, T. Gevers, and A. Gijsenij, "Edge-based color constancy," *IEEE Trans. Image Process.*, vol. 16, no. 9, pp. 2207–2214, 2007.
- [23] W. Song, Y. Wang, D. Huang, A. Liotta, and C. Perra, "Enhancement of underwater images with statistical model of background light and optimization of transmission map," *IEEE Trans. Broadcast.*, vol. 66, no. 1, pp. 153–169, 2020.
- [24] X. Fu, Z. Fan, M. Ling, Y. Huang, and X. Ding, "Two-step approach for single underwater image enhancement," in *Proc. ISPACS*. IEEE, 2017, pp. 789–794.
- [25] Z. Mi, Y. Li, Y. Wang, and X. Fu, "Multi-purpose oriented real-world underwater image enhancement," *IEEE Access*, vol. 8, pp. 112957–112968, 2020.
- [26] M. Yang and A. Sowmya, "An underwater color image quality evaluation metric," *IEEE Trans. Image Process.*, vol. 24, no. 12, pp. 6062–6071, 2015.
- [27] R. Liu, X. Fan, M. Zhu, M. Hou, and Z. Luo, "Real-world underwater enhancement: Challenges, benchmarks, and solutions under natural light," *IEEE Trans. Circuits Syst. Video Technol.*, vol. 30, no. 12, pp. 4861–4875, 2020.
- [28] Y.-T. Peng, K. Cao, and P. C. Cosman, "Generalization of the dark channel prior for single image restoration," *IEEE Trans. on Image Process.*, vol. 27, no. 6, pp. 2856–2868, 2018.
- [29] Q. Zhu, J. Mai, and L. Shao, "A fast single image haze removal algorithm using color attenuation prior," *IEEE Trans. Image Process.*, vol. 24, no. 11, pp. 3522–3533, 2015.
- [30] J. Shin, M. Kim, J. Paik, and S. Lee, "Radiance–reflectance combined optimization and structure-guided l_0 -norm for single image dehazing," *IEEE Trans. on Multi.*, vol. 22, no. 1, pp. 30–44, 2019.
- [31] S. Salazar-Colores, I. Cruz-Aceves, and J.-M. Ramos-Arreguin, "Single image dehazing using a multilayer perceptron," *J. Electron. Imaging*, vol. 27, no. 4, p. 043022, 2018.
- [32] X. Qin, Z. Wang, Y. Bai, X. Xie, and H. Jia, "Ffa-net: Feature fusion attention network for single image dehazing," in *Proc. AAAI*, vol. 34, no. 07, 2020, pp. 11908–11915.
- [33] Y. Cho, J. Jeong, and A. Kim, "Model-assisted multiband fusion for single image enhancement and applications to robot vision," *IEEE Robot. Autom. Lett.*, vol. 3, no. 4, pp. 2822–2829, 2018.
- [34] F. Crete, T. Dolmire, P. Ladret, and M. Nicolas, "The blur effect: perception and estimation with a new no-reference perceptual blur metric," in *Human vision and electronic imaging XII*, vol. 6492, 2007, p. 649201.
- [35] N. Hautiere, J.-P. Tarel, D. Aubert, and E. Dumont, "Blind contrast enhancement assessment by gradient ratioing at visible edges," *Image Anal. Stereol.*, vol. 27, no. 2, pp. 87–95, 2008.
- [36] D. Berman, T. Treibitz, and S. Avidan, "Diving into haze-lines: Color restoration of underwater images," in *Proc. BMVC*, vol. 1, no. 2, 2017.
- [37] C.-Y. Li, J.-C. Guo, R.-M. Cong, Y.-W. Pang, and B. Wang, "Underwater image enhancement by dehazing with minimum information loss and histogram distribution prior," *IEEE Trans. Image Process.*, vol. 25, no. 12, pp. 5664–5677, 2016.
- [38] Y. Wang, N. Li, Z. Li, Z. Gu, H. Zheng, B. Zheng, and M. Sun, "An imaging-inspired no-reference underwater color image quality assessment metric," *Comput. Electr. Eng.*, vol. 70, pp. 904–913, 2018.